Surface plasmon enhanced energy transfer between donor and acceptor CdTe nanocrystal quantum dot monolayers

*Manuela Lunz[1], Valerie A. Gerard[2], Yurii K. Gun'ko[2], Vladimir Lesnyak[3], Nikolai Gaponik[3], Andrei S. Susha[4], Andrey L. Rogach[4] and A. Louise Bradley[1]**

[1] Semiconductor Photonics Group, School of Physics, Trinity College Dublin, Dublin 2, Ireland

[2] School of Chemistry, Trinity College Dublin, Dublin 2, Ireland

[3] Physical Chemistry, TU Dresden, Bergstr. 66b, 01062 Dresden, Germany

[4] Department of Physics and Materials Science & Centre for Functional Photonics (CFP), City University of Hong Kong, Hong Kong, China

* corresponding author: bradlel@tcd.ie (A. L. Bradley)

RECEIVED DATE (to be automatically inserted after your manuscript is accepted if required according to the journal that you are submitting your paper to)

TOC Graphic for SP enhanced FRET between CdTe QD monolayers

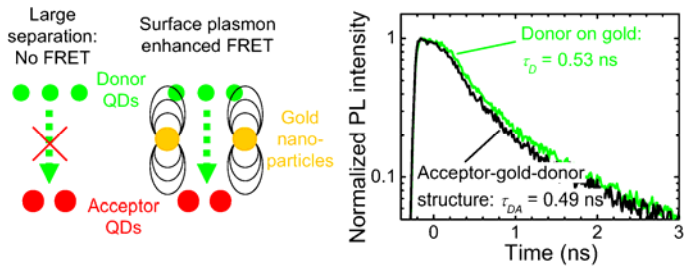

ABSTRACT: Surface plasmon enhanced Förster resonant energy transfer (FRET) between CdTe nanocrystal quantum dots (QDs) has been observed in a multilayer acceptor QD – gold nanoparticle – donor QD sandwich structure. Compared to a donor-acceptor QD bilayer structure without gold nanoparticles, the FRET rate is enhanced by a factor of 80 and the Förster radius increases by 103%. Furthermore, a strong impact of the donor QD properties on the surface plasmon mediated FRET is reported.

KEYWORDS: Quantum dots, Nanocrystals, Colloidal metal nanoparticles, Localised surface plasmons, Förster resonant energy transfer

Förster resonant energy transfer (FRET) is a non-radiative energy transfer process based on dipole-dipole interactions[1] which has been proposed as the working mechanism for different applications. Nanosensors based on the FRET mechanism have been demonstrated[2 - 4] and it has been shown that FRET can be used for color tuning or the generation of white-light emitting structures.[5 - 8] Furthermore, light-harvesting structures have been designed based on FRET,[9, 10] which could be implemented as part of detectors or photovoltaic structures. Quantum dots (QDs) have proven to be valuable components for the afore-mentioned structures due to their unique and most importantly size-tunable optical properties.[11, 12] However, due to the strong distance-dependence of the FRET process, the relatively large QD diameter, which increases the donor-acceptor centre-to-centre separation, is limiting the FRET efficiency that can be achieved in the different QD structures.[3, 13, 14] Furthermore, the inhomogeneous broadening of the QD ensemble has to be considered:[13] the size distribution present in a colloidal nanocrystal ensemble can lead to intra-ensemble energy transfer[15, 16] which can also cause a decrease in the measured donor-acceptor FRET efficiency.[17]

Localized surface plasmons (LSPs) supported by metal nanoparticles (NPs) have been successfully applied to enhance the emission of single luminescent species.[18 - 22] It has also been predicted that LSPs can enhance FRET between donors and acceptors.[23 - 25] Therefore, including metal NPs in QD - FRET structures could overcome the drawback of the QD size and improve the performance of FRET devices by increasing the FRET interaction distance, resulting in higher sensitivities and enhanced efficiencies. First experimental reports on LSP enhanced FRET between dyes give an enhancement of the FRET efficiency by a factor of approximately four and an increase of the Förster radius by almost 50%.[26, 27] A recent article by Lessard-Viger et al.[28] reports an increase of the Förster radius by 70% for the energy transfer from a conjugated polymer to a fluorescent core-shell NP with a silver core. They calculate a 12.5-fold enhancement of the FRET efficiency with a 173-fold increase of the FRET rate. Experiments on FRET in mixed donor-acceptor QD layers near gold NPs indicate an increase of the FRET efficiency by a factor of 2.7 for CdTe QD donors and acceptors[29] and a doubling in the case of CdSe/ZnS type I and CdSe/ZnTe type II core-shell QDs[30] for gold NPs with diameters of approximately 7 and 20 nm,

respectively. Furthermore, experiments with CdSe/ZnS QD donors and acceptors deposited on top of silver NPs with a diameter of 110 nm show that a large acceptor emission enhancement, in this case by a factor of 21.2, is possible in metal NP – QD FRET structures compared to the structure without metal NPs.[31] However, the presence of metal NPs can also result in a decrease of FRET between donor and acceptor species,[32] which is why it is necessary to understand well the mechanism of the LSP enhancement for its implementation in device structures. For the analysis of LSP enhanced FRET, it is necessary to differentiate between the direct impact of the metal NPs on the donor and acceptor luminescence and the actual effect of the LSPs on the energy transfer. Therefore, it is critical to characterize the QD - metal NP interaction, in order to quantify the effect of the metal NPs on the FRET process and to determine the condition for a maximum enhancement of the FRET process.

Most LSP - FRET systems including QDs as donors and acceptors studied so far were mixed donor-acceptor films deposited in proximity to metal NPs.[29 - 31] The positioning of donor and acceptor QDs on opposite sides of the metal NPs has however been predicted to be more favorable for a large LSP enhanced FRET rate.[25] Here, we present a detailed analysis of LSP mediated FRET in a multilayer acceptor QD – gold NP – donor QD sandwich structure. The steady-state as well as time-resolved photoluminescence measurements are compared to reference samples and the enhanced FRET rate, efficiency and Förster radius in the sandwich structure are determined. Furthermore, the impact of the donor QD properties on the LSP mediated FRET process is discussed for a study of six different donor QDs.

The structures were prepared by a layer-by-layer assembly technique and consisted of monolayers of donor and acceptor QDs and gold NPs separated by polyelectrolyte (PE) spacer layers. The PE layer thicknesses were validated using X-ray diffraction measurements. Details on the sample preparation and the solution concentrations of polyelectrolytes as well as CdTe QDs used for the deposition can be found elsewhere.[16, 17] Negatively charged CdTe QDs, stabilized by thioglycolic acid in aqueous solution,[33, 34] with a diameter of 2.5 nm and 3.3nm (determined from the QD absorption spectra in solution)[35] were used as donor and acceptor QDs, respectively. Positively charged colloidal gold NPs, with an average diameter of 5.5 nm and stabilized by DMAP,[36] were used to study the influence of LSPs

on FRET between donor and acceptor QDs. Gold NPs of this size can be well processed by LbL into densely packed monolayers. This allows for the preparation of a well-defined structure with well-defined vertical distances, which would not be possible for larger gold nanoparticles. Larger gold particles are typically synthesised using a different method with a different ligands (citrate) which produces a much lower concentration of gold NPs in solution and consequently, low-density monolayers using LbL deposition. This leads to a rough layer topology and a distribution of donor-acceptor separations in a multilayer structure which is unsuitable for FRET studies.

All layer structures presented here were deposited on a PE buffer layer (thickness approximately 12 nm) on quartz. To prepare the sandwich structure (a schematic of which is included in Fig. 2(a)), first a complete monolayer of acceptor QDs was deposited and covered with a PE spacer layer with a thickness of approximately 12 nm. Subsequently, a gold NP layer was deposited, followed by a thinner PE spacer (thickness 3 nm) and finally the structure was completed with the donor QD monolayer. Therefore, the donor and acceptor layers are separated by ~20.5 nm $(12\,\text{nm} + 5.5\,\text{nm} + 3\,\text{nm})$ in the sandwich structure, corresponding to a donor-acceptor centre-to-centre separation of ~23.4 nm $(20.5\,\text{nm} + 2.5\,\text{nm}/2 + 3.3\,\text{nm}/2)$. Reference structures with single donor / acceptor monolayers, donor / acceptor monolayers on gold NP layers (with PE spacer thicknesses of 3 and 12 nm, respectively) as well as donor-acceptor bilayer reference structures (with an intermediate PE spacer thickness of 21 nm, corresponding to a donor-acceptor centre-to-centre separation of ~24 nm) were also prepared for comparison with the sandwich structure. The donor-gold NP and acceptor-gold NP separations where selected based on a study of the separation dependence of the donor PL lifetime and the acceptor PL emission. The asymmetric structure reported in this letter, with an acceptor-gold separation of 12 nm and a gold-donor separation of 3 nm, showed signatures for the largest LSP enhancement of FRET between a donor and acceptor QD layer, namely the largest reduction in the donor PL lifetime and increased acceptor PL emission.

Room-temperature, steady-state photoluminescence (PL) spectra of the layer structures were recorded with a Perkin-Elmer LS 55 fluorescence spectrometer using an excitation wavelength of 400 nm,

provided by a pulsed Xenon lamp. Absorption spectra were measured with a double beam UV-Vis Spectrometer (Shimadzu UV-2401 PC). Figure 1 shows the PL spectra (left-hand axis) of a reference donor (solid green squares) and acceptor monolayer (open red circles). The absorption spectra of the donor monoloayer (green line), acceptor monolayers (red line) and gold NP layer are also included. It can be clearly seen that the donor emission, centered around 559 nm, overlaps well with the first acceptor absorption peak at 565 nm, enabling efficient resonant energy transfer between the donor and acceptor QDs. The Förster radius calculated from this spectral overlap, including a donor quantum yield of 10%, is $R_0 = (3.9 \pm 0.2)\,\text{nm}$.[17] Furthermore, the gold NP absorption peak at 532 nm, arising from the LSP resonance, also overlaps with the acceptor absorption and the donor emission.

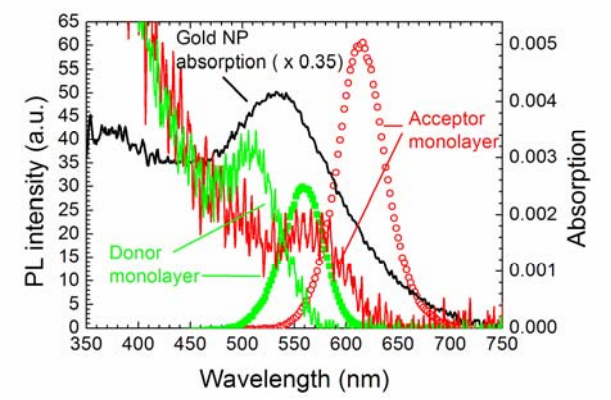

Figure 1. Photoluminescence (PL) spectra (left-hand axis) of donor (solid green squares) and acceptor (open red circles) QD monolayers deposited on quartz, with concentrations of $c_{Don} = (1.8 \pm 0.2) \times 10^{17}\,\text{m}^{-2}$ and $c_{Acc} = (0.63 \pm 0.10) \times 10^{17}\,\text{m}^{-2}$ respectively. The absorption spectra (right-hand axis) of the donor (green line) and acceptor (red line) monolayer as well as of a gold nanoparticle (NP) layer (black line), with a concentration of $c_{Au} = (0.084 \pm 0.010) \times 10^{17}\,\text{m}^{-2}$, are also shown.

The PL spectrum of a completed acceptor-gold-donor sandwich structure (solid black triangles) is shown in Fig. 2(a). The spectrum of the structure prior to depositing the PE and the donor QD monolayer on top of the gold NP layer is also shown (solid red line). As can be seen the gold NP

deposition on top of the acceptor QDs, covered with the 12 nm PE spacer, completely quenches the emission of the acceptor QDs and the remaining detected luminescence is attributed to PE emission[37] from the buffer and spacer layers. Acceptor emission is recovered for the completed sandwich structure, indicating that quenching of the acceptor PL due to the gold NPs is overcome by energy transfer from the donor to the acceptor QDs via the gold NPs.

For comparison the PL spectra of donor (open green squares) and acceptor monolayers (open red circles) on a gold NP layer are also shown. Furthermore, the spectrum of an acceptor-donor bilayer structure with a donor-acceptor centre-to-centre separation of 24 nm, is also included. As confirmed in a previous study with these QDs, at such a large separation no FRET between the donor and acceptor QDs is expected or observed.[17]

With reference to the bilayer structure without gold NPs, the donor and acceptor emission in the sandwich structure is slightly quenched, by 34% and 13% respectively, due to the presence of the gold NPs. In all cases the PL quenching is calculated from the integrated de-convolved donor/acceptor spectra. However, in comparison with the QD on gold reference structures, it can be clearly seen that the donor emission in the sandwich structure is reduced, by 13%, while the emission of the acceptors is increased by 24%. This indicates that, despite the large donor-acceptor centre-to-centre separation of 23 nm, energy is transferred from the donors to the acceptors via the FRET mechanism, even though no FRET is observed in a similar structure without gold NPs.[17] Due to the large NP separations, tunneling[38, 39] can be excluded as energy transfer mechanism. Furthermore, only donor and acceptor PL quenching has been observed for these QDs and gold NPs, as can be seen by comparing the PL spectra of the donor and acceptor monolayers on quartz and gold shown in Figs. 1 and 2(a), respectively. This excludes the misinterpretation of a direct donor or acceptor PL enhancement by the LSPs as increased energy transfer. Moreover, enhanced radiative energy transfer can be neglected as no direct enhancement of the acceptor emission for excitation wavelengths in the region of the donor emission has been observed in the acceptor PLE spectra for the acceptor QD monolayer on gold samples (data not shown).

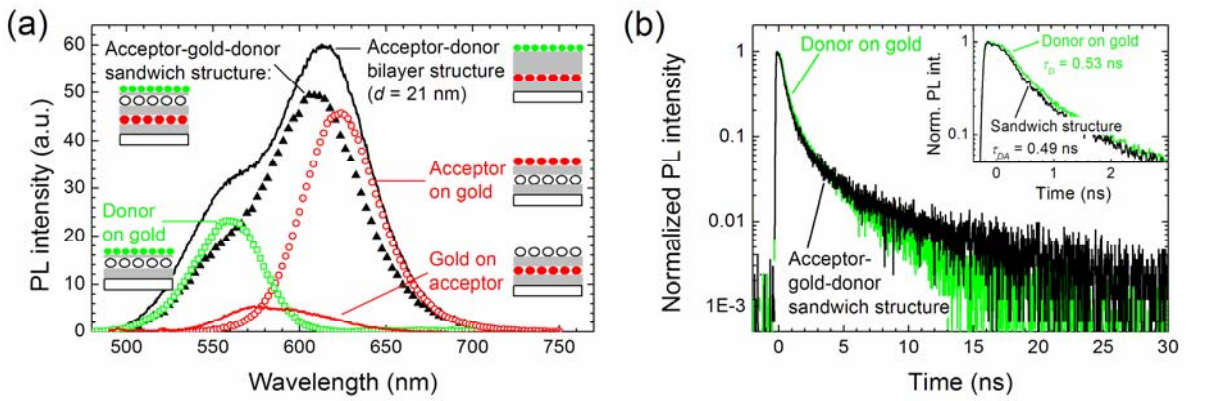

Figure 2. (a) Photoluminescence (PL) spectrum of an acceptor-gold-donor sandwich structure (black triangles) with a gold concentration $c_{Au} = (0.086 \pm 0.010) \times 10^{17}\,\mathrm{m}^{-2}$ and QD concentrations of $c_{Don} = (1.8 \pm 0.2) \times 10^{17}\,\mathrm{m}^{-2}$ and $c_{Acc} = (0.63 \pm 0.10) \times 10^{17}\,\mathrm{m}^{-2}$ for the donor and acceptor QDs respectively. The PL spectrum of the sandwich structure prior to the deposition of the final polyelectrolyte and donor QD monolayer is also shown (red line). For comparison the PL spectra of donor monolayers (open green squares) and acceptor monolayers (open red circles) deposited on top of a gold nanoparticle layer as well as a donor-acceptor bilayer structure without gold nanoparticles (black line) are also included. The acceptor PL in the gold on acceptor structure is lower than that measured from the acceptor on gold reference structure due to absorption of the incident excitation light and the acceptor emission by both the PE layers and gold nanoparticles on top of the buried acceptor QD monolayer. In the bilayer structure the donor and acceptor concentrations are $c_{Don} = (2.4 \pm 0.2) \times 10^{17}\,\mathrm{m}^{-2}$ and $c_{Acc} = (0.67 \pm 0.10) \times 10^{17}\,\mathrm{m}^{-2}$ respectively. The schematics show the layer structures of the different samples prepared on quartz (white rectangle). The polyelectrolyte spacer layers are indicated in grey; the red, white and green spheres represent the acceptor QDs, gold nanoparticles and donor QDs respectively. (b) Time-resolved donor PL decays for the donor on gold reference (green line) and the acceptor-gold-donor sandwich structure (black line). The inset shows a close-up of these two donor PL decays over the first three nanoseconds. The time-resolved PL decays were measured at 500 nm using a broad band-filter with a full width at half maximum of approximately $(70 \pm 5)\,\mathrm{nm}$.

Further confirmation of LSP mediated FRET as the origin of the observed donor and acceptor PL signatures is found in the time-resolved donor PL decays shown in Fig. 2(b). The time-resolved PL decays were measured with a PicoQuant Mictotime 200 time-resolved confocal microscope with 150 ps time resolution. A LDH-480 laser head, controlled by a PDL-800B driver (PicoQuant), provided picosecond excitation pulses at 470 nm with an average power of 16 nW. The PL decays were measured over an area of 80 x 80 μm^2 (150 x 150 pixels) with a repetition rate of 10 MHz and an integration time of 4 ms per pixel. A 500 nm broad band-filter with a full width at half maximum of approximately (70 ± 5) nm was used to investigate the emission from the donors only. In the main panel of Fig. 2(b) the donor PL decay of the sandwich structure as well as that of the donor on gold reference structure can be seen. The overall decays are very similar, but the close-up over the first three nanoseconds, shown in the inset, reveals a faster initial decay of the donor QDs in the sandwich structure when compared with the donor QD on gold NP layer structure. This change in PL decay provides further evidence that energy is transferred from the donors to the acceptors by the FRET mechanism despite the large donor-acceptor separation.

A comparison of the short lifetime component extracted from a multi-exponential fit of the donor PL decays for the sandwich structure, $\tau_{DA} = (0.49 \pm 0.01)$ ns, with that for the donor on gold reference sample, $\tau_D = (0.53 \pm 0.01)$ ns, indicates that energy is transferred from the donors to the acceptors at a rate of $k_{\mathrm{FRET}} = {\tau_{DA}}^{-1} - {\tau_D}^{-1} = (6.5\,\mathrm{ns} \pm 2.3\,\mathrm{ns})^{-1}$ and with an efficiency of $E_{\mathrm{FRET}} = 1 - \tau_{DA}/\tau_D = (8 \pm 2)\%$. The FRET efficiency determined from the donor lifetime decrease is in relatively good agreement with the donor PL quenching of 13%.

The rate k_{FRET} and efficiency E_{FRET} of FRET between two planes[17] can be calculated using equations (1) and (2) respectively:

$$k_{\mathrm{FRET}} = \frac{c_{\mathrm{Acc}} \pi {R_0}^6}{2 d^4 \tau_D} \qquad (1)$$

$$E_{\mathrm{FRET}} = \frac{1}{1 + \frac{2d^4}{c_{\mathrm{Acc}} \pi R_0^{\,6}}} \quad . \qquad (2)$$

Including a Förster radius $R_0 = (3.9 \pm 0.2)\,\mathrm{nm}$ and a short donor lifetime component $\tau_D = (0.60 \pm 0.01)\,\mathrm{ns}$ (measured for the bilayer and donor monolayer), in equations (1) and (2) a FRET rate of $k_{\mathrm{FRET}} = (517\,\mathrm{ns} \pm 230\,\mathrm{ns})^{-1}$ and an efficiency of $(0.12 \pm 0.05)\%$ are obtained for a structure without the gold NP layer but with the same donor-acceptor centre-to-centre separation $d = (23.4 \pm 1.7)\,\mathrm{nm}$ and acceptor concentration $c_{Acc} = (0.63 \pm 0.10) \times 10^{17}\,\mathrm{m}^{-2}$ as in the sandwich structure. Due to the strong dependence of the FRET efficiency and FRET rate on the donor-acceptor separation and Förster radius even small errors in the estimation of these parameters can result in a large uncertainty in the estimated FRET efficiency and rate. However, the relative change in the FRET rate (by a factor of (80 ± 45)) and efficiency between the bilayer and sandwich structure is still significant and manifests as a large increase of the Förster radius.

Based on equations (1) and (2), one can calculate the Förster radius for the transfer process that would lead to the efficiency and rate observed in the sandwich structure taking into account $d = (23.4 \pm 1.7)\,\mathrm{nm}$ and $c_{Acc} = (0.63 \pm 0.10) \times 10^{17}\,\mathrm{m}^{-2}$ as well as a donor lifetime of $\tau_D = (0.53 \pm 0.01)\,\mathrm{ns}$, measured for the donor monolayer on gold. The Förster radius in the sandwich structure obtained with equations (1) as well as (2) is $(7.9 \pm 0.5)\,\mathrm{nm}$, which is double the value determined from the spectral overlap, $R_0 = (3.9 \pm 0.2)\,\mathrm{nm}$, in the QD bilayer structure without gold NPs. To our knowledge, this is the largest increase of the Förster radius by LSPs reported to date. Due to the presence of the gold NPs the FRET rate is enhanced and therefore the distance over which FRET can occur is largely increased. Including metal NPs into QD-FRET structures therefore represents a means to improve the performance of devices and provide greater flexibility in the QD-FRET device design as larger separations between donor and acceptor components can be tolerated.

In the following, the impact of donor QD properties on FRET in sandwich structures is presented. The PL spectra of the donor QDs (A-F) used are shown as coloured lines in Fig. 3. As can be seen the emission spectra of the different QDs overlap with the relatively broad LSP absorption peak, also shown in Fig. 3 (black line, right hand axis). The QDs have a range of central peak emission wavelengths and quantum yields. Further details on the properties of these donor QDs are given in Table 1. The quantum yields of the QDs in the monolayers were determined by a relative calculation,[40] comparing their absorption and emission properties to those of the luminescent standard Rhodamine 6G. The Don-C QDs have been used as donors for the preparation for the samples discussed earlier. Don-C has the largest quantum yield in a monolayer, while Don-A and Don-B show the strongest interaction with the gold NPs, indicated by a large PL and lifetime quenching when deposited on a gold NP layer.

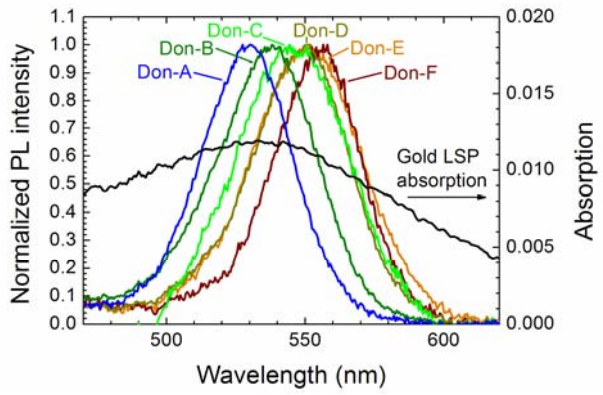

Figure 3. Normalized photoluminescence (PL) spectra (left-hand axis) of six different donor QDs (Don-A to F). To visualize the overlap with the localized surface plasmon (LSP) absorption feature of the colloidal gold nanoparticles (NPs), the absorption spectrum recorded for a gold NP layer with a concentration of $c_{Au} = (0.084 \pm 0.010) \times 10^{17}\,\mathrm{m}^{-2}$ is also shown (right-hand axis).

Table 1. Properties of the donor QDs: central emission wavelength (nm) and quantum yield of the donor QD monolayers (MLs) on quartz as well as PL quenching $(1 - I_{onAu}/I_{ref})$ and lifetime reduction $(1 - \tau_{onAu}/\tau_{ref})$ of the donor MLs on a gold nanoparticle layer with a concentration of $c_{Au} = (0.09 \pm 0.02) \times 10^{17}\,\mathrm{m}^{-2}$:

Donors	A	B	C	D	E	F
Central emission wavelength (nm)	533	538	546.5	547.8	553.5	556.4
Quantum yield	6%	6%	10%	3%	5%	2%
PL quenching on gold	64%	57%	25%	0%	15%	0%
Lifetime decrease on gold	51%	48%	28%	39%	51%	26%

In Figure 4, the PL spectra of the full sandwich structures are presented for the different donor QDs investigated. Donor emission is visible for all sandwich structures, but a PL signal in the wavelength range of the acceptor emission is only detected for sandwich structures including Don-A, Don-B and Don-C QDs. No acceptor PL is observed for sandwich structures with Don-D, Don-E and Don-F QDs. The acceptor QD concentration was similar for all sandwich structures, and therefore the acceptor emission can be used as an indicator of FRET. The donor quantum yield appears to play an important role in LSP mediated FRET, as the largest acceptor emission is observed for the sandwich structure with Don-C, the donor QDs with the largest quantum yield of 10% in the monolayer. The emission quenching and decrease of the lifetime for donor QDs deposited on the gold monolayer can be considered as an indicator of the strength of the QD - gold interaction. All QDs investigated showed a decrease (given as $1-\tau_{onAu}/\tau_{ref}$ in Table 1) of the lifetime measured for the monolayer deposited on gold τ_{onAu}, compared to the reference lifetime τ_{ref}, determined for a QD monolayer on quartz. The PL quenching, $1-I_{onAu}/I_{ref}$, calculated from the spectrally integrated PL emission I_{onAu} for the donor monolayer on gold and I_{ref} of the reference monolayer deposited on quartz, is also summarized in Table 1. Comparing for example Don-A, Don-B and Don-E, only sandwich structures with Don-A and Don-B show an acceptor emission even though Don-E has a similar quantum yield to Don-A and Don-B. However, the peak emission wavelength for Don-E is shifted to the red with respect to the central wavelength of the LSP peak absorption and it also shows a smaller PL quenching, suggesting a weaker interaction with the LSPs than QDs Don-A and Don-B. Don-D and Don-F also don't show evidence for LSP mediated FRET. It can be noted that their quantum yield is low and the interaction with the gold

NPs is weaker, as indicated by the lack of PL quenching. This clearly shows that the donor QD properties, in particular the quantum yield and the emission wavelength, can strongly influence the efficiency of LSP mediated FRET.

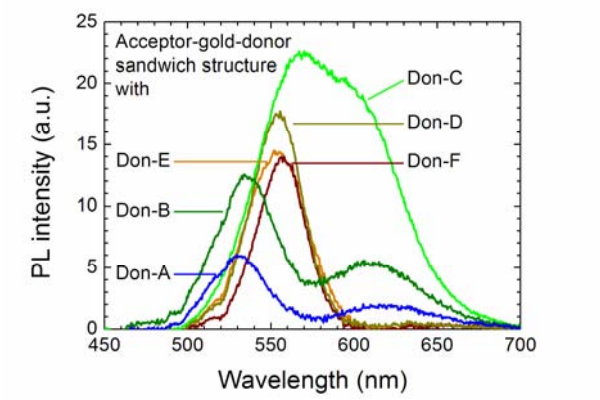

Figure 4. Photoluminescence (PL) spectra of acceptor-gold-donor sandwich structures prepared with six different CdTe QDs (Don-A to F). The donor and acceptor concentrations as well as that of the gold nanoparticles, $c_{Au} = (0.09 \pm 0.02) \times 10^{17}\,\mathrm{m}^{-2}$, were similar for all samples.

In conclusion, we have presented clear evidence for surface plasmon enhanced FRET in a QD - metal NP sandwich structure, consisting of donor QD, gold NP and acceptor QD monolayers separated by polyelectrolyte spacer layers. A FRET efficiency of 8% was determined for a donor-acceptor centre-to-centre separation of 23.4nm, a distance over which the FRET efficiency is expected to be almost zero (0.12%) in the absence of the gold NP layer. The FRET rate of $k_{\mathrm{FRET}} = (6.5\,\mathrm{ns})^{-1}$ in the sandwich structure represents a 80-fold increase over what is expected for a structure without gold NPs, corresponding to a doubling of the Förster radius from 3.9 nm to 7.9 nm. This clearly shows that by including metal NPs into QD FRET structures, the FRET efficiency can be enhanced and the distance over which it occurs can be significantly increased. This opens up possibilities for new designs of QD - FRET structures and provides a way to improve the performance of QD - FRET devices. Furthermore, it was shown that the donor properties have a large impact on the probability for surface plasmon mediated FRET. Donors with PL emission spectra in resonance with the surface plasmon absorption peak of gold NP monolayers showed a clear signature of surface plasmon mediated energy transfer,

reflected in a large acceptor emission, in contrast to those donor QDs with an emission shifted slightly to the red. Additionally, the largest acceptor emission enhancement was achieved for donor QDs with the highest quantum yield.

ACKNOWLEDGMENT We thank Robert Gunning for the thickness measurements of the polyelectrolyte layers by X-ray diffraction. This work was financially supported by Science Foundation Ireland projects 05/PICA/1797, 07/IN.1/I1862 and 10/IN.1/12975.

REFERENCES:

(1) Förster, T. *Annalen der Physik* **1948**, *2*, 55

(2) Miyawaki, A.; Llopis, J.; Heim, R.; McCaffery, J. M.; Adams, J. A.; Ikura, M.; Tsien, R. Y. *Nature* **1997**, *388*, 882

(3) Medintz, I. L.; Clapp, A. R.; Mattoussi, H.; Goldman, E. R.; Fisher, B.; Mauro, J. M. *Nature Mater.* **2003**, *2*, 630

(4) Willard, D. M.; Mutschler, T.; Yu, M.; Jung, J.; Van Orden, A. *Anal. Bioanal. Chem.* **2006**, *384*, 564

(5) Achermann, M.; Petruska, M. A.; Kos, S.; Smith, D. L.; Koleske, D. D.; Klimov, V. I. *Nature* **2004**, *429*, 6992

(6) Cicek, N.; Nizamoglu, S.; Ozel, T.; Mutlugun, E.; Karatay, D. U.; Lesnyak, V; Otto, T.; Gaponik, N.; Eychmüller, A.; Demir, H. V. *Appl. Phys. Lett.* **2009**, *94*, 061105

(7) Chanyawadee, S.; Lagoudakis, P. G.; Harley, R. T.; Charlton, M. D. B.; Talapin, D. V.; Huang, H. W.; Lin, C. H. *Adv. Mater.* **2010**, *22*, 602

(8) Nizamoglu, S.; Sari, E.; Baek, J. H.; Lee, I. H.; Demir, H. V. *New J. Phys.* **2004**, *10*, 123001

(9) Franzl, T.; Klar, T. A.; Schietinger, S.; Rogach, A. L.; Feldmann, J. *Nano Lett.* **2004**, *4*, 1599

(10) Lee, J.; Govorov, A. O.; Kotov, N. A. *Nano Lett.* **2005**, *5*, 2063

(11) Gaponenko, S. V. *Optical properties of semiconductor nanocrystals*; Cambridge University Press: Cambridge, 1998

(12) Rogach, A. L. *Semiconductor nanocrystals quantum dots: synthesis, assembly, spectroscopy and applications*; Springer: Wien, 2008

(13) Scholes, G. D.; Andrews, D. L. *Phys. Rev. B* **2005** *72*, 125331

(14) Lunz, M.; Bradley, A. L.; Chen, W.-Y.; Gun'ko, Y. P. *J. Phys. Chem. C* **2009**, *113*, 3084

(15) Kagan, C. R.; Murray, C. B.; Bawendi, M. G. *Phys. Rev. B* **1996**, *54*, 8633

(16) Lunz, M.; Bradley, A. L.; Chen, W.-Y.; Gerard, V. A.; Byrne, S. J.; Gun'ko, Y. P.; Lesnyak, V.; Gaponik, N. *Phys. Rev. B* **2010**, *81*, 205316

(17) Lunz, M.; Bradley, A. L.; Gerard, V. A.; Byrne, S. J.; Gun'ko, Y. P.; Lesnyak, V.; Gaponik, N. *Phys. Rev. B* **2011**, *83*, 115423

(18) Kulakovich, O.; Strekal, N.; Yaroshevich, A.; Maskevich, S.; Gaponenko, S.; Nabiev, I.; Woggon, U.; Artemyev, M. *Nano Lett.* **2002**, *2*, 1449

(19) Anger P.; Bharadwaj, P.; Novotny, L. *Phys. Rev. Lett.* **2006**, *96*, 113002

(20) Komarala, V. K.; Rakovich, Y. P.; Bradley, A. L.; Byrne, S. J.; Gun'ko, Y. P.; Gaponik, N.; Eychmüller, A. *Appl. Phys. Lett.* **2006**, *89*, 253118

(21) Pompa, P. P.; Martiradonna, L.; Della Torre, A.; Della Sala, F.; Manna, L; De Vittorio, M.; Calabi, F.; Cingolani, R.; Rinaldi, R. *Nature Nanotech.* **2006** , *1*, 126

(22) Bek, A.; Jansen, R.; Ringler, M.; Mayilo, S.; Klar, T. A.; Feldmann, J. *Nano Lett.* **2008**, *8*, 485

(23) Gersten, J. I.; Nitzan, A. *Chem. Phys. Lett.* **1984**, *104*, 31

(24) Hua, X. M.; Gersten, J. I.; Nitzan, A. *J. Chem. Phys.* **1985**, *83*, 3650

(25) Govorov, A. O.; Lee, J.; Kotov, N. A. *Phys. Rev. B* **2007**, *76*, 125308

(26) Zhang, J.; Fu, Y.; Lakowicz, J. R. *J. Phys. Chem. C* **2007**, *111*, 50

(27) Lessard-Viger, M.; Rioux, M.; Rainville, L.; Boudreau, D. *Nano Letters* **2009**, *9*, 3066

(28) L.-Viger, M.; Brouard, D., Boudreau, D. *J. Phys. Chem. C* **2011**, *115*, 2974

(29) Komarala, V. K.; Bradley, A. L.; Rakovich, Y. P.; Byrne, S. J.; Gun'ko, Y. K.; Rogach, A. L. *Appl. Phys. Lett.* **2008**, *93*, 123102

(30) Wang, C. H.; Chen, C. W.; Chen, Y. T.; Wei, C. M.; Chen, Y. F.; Lai, C. W.; Ho, M. L.; Chou, P. T.; Hofmann, M. *Appl. Phys. Lett.* **2010**, *96*, 071906

(31) Su, X. R.; Zhang, W.; Zhou, L.; Peng, X. N.; Pang, D. W.; Liu, S. D.; Zhou, Z. K.; Wang, Q. Q. *Appl. Phys. Lett.* **2010**, *96*, 043106

(32) Reil, F.; Hohenester, U.; Krenn, J. R.; Leitner, A. *Nano Letters* **2008**, *8*, 4128

(33) Byrne, S. J.; Corr, S. A.; Rakovich, T. Y.; Gun'ko, Y. K.; Rakovich, Y. P.; Donegan, J. F; Mitchell, S.; Volkov, Y. *J. Mater. Chem.* **2006**, *16*, 2896

(34) Rogach, A. L.; Franzl, T.; Klar, T. A.; Feldmann, J.; Gaponik, N.; Lesnyak, V.; Shavel, A.; Eychmüller, A.; Rakovich, Y. P.; Donegan, J. F. *J. Phys. Chem. C* **2007**, *111*, 14628

(35) Yu, W. W.; Qu, L. H.; Guo, W. Z.; Peng, X. G. *Chem. Mater.* **2003**, *15*, 2854

(36) Gittins, D. I.; Caruso, F. *Angew. Chem. - Int. Ed.* **2001**, *40*, 3001

(37) Reilly, R. S.; Smyth, C. A.; Rakovich, Y. P.; McCabe, E. M. *Nanotechnology* **2009**, *20*, 095707

(38) Dexter, D. L. *J. Chem. Phys.* **1953**, *21*, 836

(39) Inokuti, M.; Hirayama, F. *J. Chem. Phys.* **1965**, *43*, 1978

(40) Fery-Forgues, S.; Lavabre, D. *Journal of Chemical Education* **1999**, *76*, 1260